Identification of Angiogenesis Inhibitors Using a Co-culture Cell Model in a High-Content and High-Throughput Screening Platform

Shuaizhang Li[1], Chia-Wen Hsu[1], Srilatha Sakamuru[1], Chaozhong Zou[2], Ruili Huang[1], and Menghang Xia[1]

Abstract

Angiogenesis is an important hallmark of cancer, contributing to tumor formation and metastasis. In vitro angiogenesis models for analyzing tube formation serve as useful tools to study these processes. However, current in vitro co-culture models using primary cells have limitations in usefulness and consistency. Therefore, in the present study, an in vitro co-culture assay system was optimized in a 1536-well format for high-throughput screening using human telomerase reverse transcriptase (hTERT)–immortalized mesenchymal stem cells and aortic endothelial cells. The National Center for Advancing Translational Sciences (NCATS) Pharmaceutical Collection (NPC) library containing 2816 drugs was evaluated using the in vitro co-culture assay. From the screen, 35 potent inhibitors ($IC_{50} \leq 1$ µM) were identified, followed by 15 weaker inhibitors (IC_{50} 1–50 µM). Moreover, many known angiogenesis inhibitors were identified, such as topotecan, docetaxel, and bortezomib. Several potential novel angiogenesis inhibitors were also identified from this study, including thimerosal and podofilox. Among the inhibitors, some compounds were proved to be involved in the hypoxia-inducible factor-1α (HIF-1α) and the nuclear factor-kappa B (NF-κB) pathways. The co-culture model developed by using hTERT-immortalized cell lines described in this report provides a consistent and robust in vitro system for antiangiogenic drug screening.

Keywords

angiogenesis, co-culture cell model, high-content screening, 1536-well plate format

Introduction

Angiogenesis is a fundamental, developmental, and physiological process of forming new blood vessels that are required for tumor formation, invasion, and metastasis. Angiogenesis has been considered a hallmark of cancer.[1] The key signaling system of angiogenesis is vascular endothelial growth factors (VEGFs) and their receptors. VEGF-targeted therapies have been a promising strategy to inhibit angiogenesis in the treatment of cancer and other related disorders.[2,3] At present, several VEGF inhibitors, such as bevacizumab, sorafenib, sunitinib, and pazopanib, have been approved by the U.S. Food and Drug Administration (FDA) for clinical use.[4–7] Angiogenesis models provide useful tools in the study of the relationship between tumor growth and angiogenesis, possibly creating new cancer therapies.

In vivo and in vitro angiogenesis assays have been summarized and reviewed.[8–10] In vivo assays are tumor angiogenesis models based on chick chorioallantoic membrane (CAM), corneal, sponge implantation, chamber, dorsal air sac, or zebrafish

assays. The commonly used in vitro angiogenesis assays include cell migration, endothelial cell (EC) proliferation, cell differentiation, co-culture with fibroblasts and mural cells, and vessel outgrowth from organ cultures. With the development of a high-throughput screening (HTS) assay, several in vitro biochemical angiogenesis-related assays have been optimized in 96- to 1536-well formats. For example, biochemical assays targeting vascular endothelial growth factor receptor (VEGFR), tumor necrosis factor α (TNF-α), tumor necrosis factor β

[1]Division of Pre-Clinical Innovation, National Center for Advancing Translational Sciences, National Institutes of Health, Bethesda, MD, USA
[2]American Type Culture Collection, Gaithersburg, MD, USA

Corresponding Author:
Menghang Xia, National Institutes of Health, National Center for Advancing Translational Sciences, 9800 Medical Center Dr., Bethesda, MD 20892, USA.
Email: mxia@mail.nih.gov

(TNF-β), hypoxia-inducible factor-1α (HIF-1α), and integrins have been applied to large-scale screenings.[11–15] In addition, several cell-based immunofluorescence or reporter gene assays have been used based on the angiogenesis-related signal pathways, such as HIF-1α, interleukin-6/interleukin-8 (IL-6/IL-8), and TGFα/β.[16–22] Compared with biochemical assays, which target artificially generated systems, cell-based HTS assays are more biologically relevant.

However, these biochemical and cell-based assays with related angiogenesis signaling pathways are not representative of a specific angiogenesis model, which may underevaluate the off-target effects. The assays using endothelial tube formation in Matrigel[8] or in egg white matrix[23] are not suitable for HTS. Tubules formed in co-culture assays were significantly heterogeneous and closely resembled capillaries than tubules in Matrigel.[8] High-content screening (HCS) technologies can be used to interrogate a biological system by combining high-throughput and cellular imaging techniques.[24] Evensen et al. developed an HCS-compatible co-culture model of primary human ECs and vascular smooth muscle cells (vSMCs) for high-throughput antiangiogenic compound screening.[25] Although additional in vitro co-culture models have been developed using primary cells, their usefulness and consistency are limited by donor variability, low cell quantity per lot, and short life span of primary cells. To overcome this, stable fluorescent EC lines based on immortalized human microvascular endothelial cells (HMECs) were employed for 96- and 384-well HTS.[26]

Selecting the appropriate in vitro cell-based angiogenesis assay for screening large numbers of chemical compounds in a quantitative high-throughput screening (qHTS) platform poses a challenge. In this study, we validated and miniaturized an in vitro co-culture model system in a 1536-well plate format using cell lines, immortalized by human telomerase reverse transcriptase (hTERT) alone. The angiogenesis co-culture model utilizes hTERT mesenchymal stem cells and hTERT-immortalized aortic ECs, which eliminates donor variability and reduces the lot-to-lot variations seen in primary cells, while offering the advantage of larger lot sizes and greater assay consistency. To validate the co-culture mode system, the assay was screened against the National Center for Advancing Translational Sciences (NCATS) Pharmaceutical Collection (NPC) library containing 2816 compounds in a qHTS platform, in which each test compound is assayed at seven concentrations. Our assay greatly reduced rates of false positives and negatives and facilitated compound prioritization for in-depth studies. Therefore, this angiogenesis assay will be useful for a wide range of angiogenesis applications in both academia and industry.

Materials and Methods

Reagents

The Angio-Ready Angiogenesis Assay Kit was obtained from the American Type Culture Collection (Manassas, VA). The hTERT-immortalized mesenchymal stem cells and aortic ECs were cultured using the medium provided in the kit supplemented with 25 U/mL penicillin and 25 μg/mL streptomycin. Sunitinib and lapatinib were obtained from Sigma-Aldrich Co. (St. Louis, MO). Recombinant human EGF was from Bio-Rad (Hercules, CA). The NPC library[27] was prepared as stock solutions in DMSO in 1536-well compound plates.

In Vitro Cell-Based Angiogenesis Co-culture Assay

The angiogenesis co-culture assay was conducted using the Angio-Ready Angiogenesis Assay according to the manufacturer's instructions. Cells were seeded in a 96-well clear-bottom plate (Corning, Oneonta, NY) for 5 h and exposed to test compounds for 3 days at 37 °C, 5% CO_2. The tube formation and cell viability of each well were acquired on an ArrayScan VTI reader (Thermo Fisher, Waltham, MA) with a 5× objective and $488_{excitation}/530_{emission}$ filters to image the green fluorescent protein (GFP)–expressing tubular structures and on a ViewLux plate reader (PerkinElmer, Waltham, MA) using CellTiter-Glo reagent (Promega, Madison, WI), respectively.

Angiogenesis Assay in a 1536-Well Plate Format

The angiogenesis assay can quantify the tubule changes in cells using an ArrayScan VTI reader. The GFP-expressing tubular structure is used to detect angiogenesis formation. Briefly, immortalized mesenchymal stem cells (hTERT-MSCs) and aortic ECs (TeloHAECs) were dispensed at 5000 cells/7.5 μL/well by using a Multidrop Combi eight-channel dispenser (Thermo Fisher) into 1536-well black-wall/clear-bottom assay plates (Aurora Microplates, Whitefish, MT). The assay plates were incubated at 37 °C for 5 h to allow cell attachment to the well bottoms, followed by the addition of 23 nL of compounds via a Wako Pintool station (Wako Automation, San Diego, CA). The final concentrations of the compounds ranged from 12 nM to 38.3 μM. Sunitinib (6.13 μM final concentration), a known angiogenesis inhibitor, was used as a positive control and DMSO was used as a negative control in the screening. The assay plates were then incubated at 37 °C for 48 h, and 5 μL of 8% paraformaldehyde (4% final concentration) fixative solution was added to each well using a microplate washer (BioTek, Winooski, VT). After incubation at room temperature (RT) for 15–30 min, the assay plates were washed once with Dulbecco's phosphate-buffered saline (DPBS) solution using a BioTek microplate washer. The assay plates were sealed and stored at 4 °C before imaging. The fluorescence intensities ($488_{excitation}/530_{emission}$ filters for GFP) were measured using an ArrayScan VTI reader (Thermo Fisher) with a 5× Plan Fluor objective (Nikon). Images were acquired for one site (a single field in a 1536-well plate) in

each well and analyzed with the HCS Studio Cell Analysis software for angiogenesis. Several algorithmic outputs, such as valid tube count and total area, were used for quantitative image analysis of angiogenesis. Cell viability after compound treatment was determined using a CellTiter-Glo viability assay by measuring intracellular adenosine triphosphate (ATP) content (Promega).

HRE-bla Reporter Gene Assay

A cell culture of HRE-bla ME-180 cells and an HRE-bla assay were performed as described previously.[28] Briefly, HRE-bla cells were seeded at 2500 cells/well in 1536-well black clear-bottom plates (Greiner Bio-One, Monroe, NC) and treated with test compounds at 37 °C, 5% CO_2, and 1% O_2 for 18 h, followed by the addition of a β-lactamase substrate CCF4 and CellTiter-Glo reagent (Promega). The fluorescence signals (405 nm excitation, 460 and 530 nm emissions) of CCF4 and the luminescence signals of CellTiter-Glo were acquired on Envision and ViewLux plate readers (PerkinElmer), respectively.

HIF-1α–NanoLuc Reporter Gene Assay

The HIF-1α–NanoLuc reporter gene assay was performed as reported previously.[29] The X-MAN HIF-1α–NanoLuc cells at 1500 cells/well in 1536-well plates were incubated with test compounds at 37 °C, 5% CO_2, and 1% O_2 for 18 h in a humidified CO_2 incubator with variable oxygen control, followed by the addition of Nano-Glo reagent or CellTiter-Glo cell viability assay reagent. The luminescence signals were collected on a ViewLux plate reader (PerkinElmer).

NF-κB β-Lactamase and Luciferase Reporter Gene Assays

Nuclear factor-kappa B (NF-κB) β-lactamase and luciferase reporter assays were performed as described previously.[30] NF-κB-bla cells or NF-kB-luc cells were dissociated with 0.05% trypsin/EDTA, resuspended in assay medium, and dispensed at 2000 cells/5 μL/well in a 1536-well black clear- or 2000 cells/4μL/well in a white solid-bottom plate (Greiner Bio-One) using a BioRAPTR Flying Reagent Dispenser (FRD) (Beckman Coulter, Pasadena, CA). Twenty-three nanoliters of compound was transferred to the assay plate by a Wako Pintool station (Wako Automation). One microliter of medium with or without 1 ng/mL TNF-α was dispensed by an FRD. After the plates were incubated for 5 h at 37 °C, 1 μL of LiveBLAzer B/G FRET substrate (Thermo Fisher) detection mixture and 5 μL of ONE-Glo luciferase assay reagent (Promega) were added. The plates were incubated at RT for 2 h and 30 min, respectively, and fluorescence intensity (405 nm excitation, 460 and 530 nm emissions) and luminescence were measured by an Envision plate reader and a ViewLux plate reader (PerkinElmer), respectively.

Data Analysis

Analysis of compound concentration–response data was performed as previously described.[31,32] Briefly, raw plate reads for each titration point were first normalized relative to the positive control compound (sunitinib) and DMSO-only wells (0%) as follows:

$$\% \text{ Activity} = \left[\left(V_{compound} - V_{DMSO} \right) / \left(V_{DMSO} - V_{pos} \right) \right] \times 100$$

where $V_{compound}$ denotes the compound well values, V_{pos} denotes the median value of the positive control wells, and V_{DMSO} denotes the median values of the DMSO-only wells. The data set was then corrected using the DMSO-only compound plates at the beginning and end of the compound plate stack by applying an in-house pattern correction algorithm. The half maximum effective values (IC_{50}) for each compound and maximum response (efficacy) values were obtained by fitting the concentration–response curves of each compound to a four-parameter Hill equation. Compounds were designated as class 1–4 according to the type of concentration–response curve observed.[31,32] In the present study, antagonists were defined as compounds that inhibited angiogenesis activity. Compounds with class −1.1, −1.2, −2.1, or −2.2 (efficacy ≤50%) curves were considered active, compounds with class 4 curves were considered inactive, and compounds with all other curve classes were defined as inconclusive. The potential angiogenesis inhibitors were also tested for purity. Data were analyzed and depicted using OriginPro 2015 (OriginLab Corp., Northampton, MA) and GraphPad Prism 5 (GraphPad Software, Inc., La Jolla, CA).

Results

Development of High-Content Angiogenesis Assay in a 1536-Well Plate Format

To find a better cell-based high-throughput angiogenesis assay system for quickly identifying compounds that inhibit angiogenesis, we optimized and validated a co-culture cell-based angiogenesis assay using a quantitative high-throughput and high-content imaging method. hTERT-MSCs were co-cultured with TeloHAECs expressing GFP, allowing for real-time visualization of angiogenesis. To validate this assay, the co-cultured cells were first plated in a 96-well plate. After 7 days in culture, the fluorescent branching structure was colocalized with the α-smooth muscle actin (αSMA) antibody. As shown in **Figure 1**, sunitinib, a known angiogenesis inhibitor, inhibited angiogenesis formation in a concentration-dependent manner in a 96-well plate
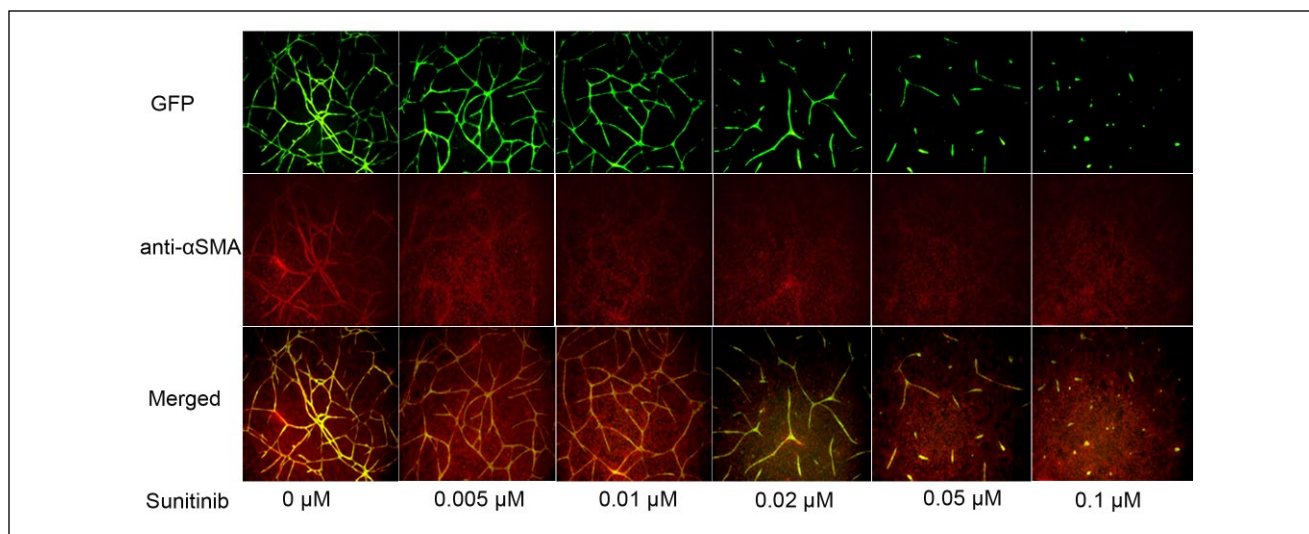
Figure 1. Establishment of an angiogenesis co-culture assay in response to sunitinib treatment. TeloHAEC-GFPs and hTERT-MSCs were co-cultured for 7 days. The co-cultured cells showed a fluorescent branching structure, which colocalized with the αSMA antibody. There were dose–response effects when the cells were treated with sunitinib, a known angiogenesis inhibitor.

format. Several measurement parameters, such as tube length, mean tube length and width ratio, valid tube count, and total tube area, were evaluated for assay performance. Of all, valid tube count and total tube area were the best-performing parameters. In a concentration-dependent manner, sunitinib inhibited angiogenesis in the co-cultured cells with IC_{50s} of 33.1 nM (**Fig. 2A**) and 24.8 nM (**Fig. 2B**) using valid tube count and total tube area measurements, respectively. After 3 days of culture in 1536-well plates, cellular images displayed spontaneous tube formation as well as sunitinib-induced tube inhibition (**Fig. 2C**). In the screening, valid tube count was used for quantitative image analysis of tube formation of angiogenesis. The co-culture assay was validated in 1536-well formats using known angiogenesis inhibitors with average signal-to-background (S/B) ratio, coefficient of variation (CV) value, and Z′ factor of 7.39, 11.5%, and 0.45, respectively.

Identification and Confirmation of Angiogenesis Inhibitors Using a qHTS Platform

To evaluate the screening performance of the high-content angiogenesis assay in a qHTS format, we screened the library for angiogenesis inhibitors in the co-culture model. Dose-response curves for 2816 compounds in the primary screening were shown in **Figure 3**. The average CV value, S/B ratio, and Z′ factor from the primary screen of 20 assay plates were 14.85 ± 5.77%, 5.53 ± 2.02, and 0.32 ± 0.14, respectively. From the primary screening, 128 potential inhibitors were identified and selected for retesting. Out of 128, 109 compounds were confirmed in the confirmation study, resulting in an 85% concordance rate between the primary screening and confirmation testing. Fifty compounds in the curve classes of −1.1, −1.2, −2.1, or −2.2

were considered active and potential angiogenesis inhibitors. Thirty-five potent inhibitors ($IC_{50} \leq 1$ μM) were identified, followed by 15 weaker inhibitors (IC_{50} 1–50 μM). In addition, most known angiogenesis inhibitors that were approved anticancer and antitumor drugs were identified in our screening, such as topotecan hydrochloride (IC_{50} 0.03 μM), docetaxel (IC_{50} 0.0025 μM), and bortezomib (IC_{50} 0.02 μM), consistent with the previous reports.[9] The known angiogenesis inhibitors and the related pathways are summarized in **Table 1**. Several potential novel inhibitors, like thimerosal and podofilox, were also identified in the screen with an IC_{50} of 0.60 and 0.03 μM, respectively. Thimerosal is commonly used as a preservative in vaccines, skin test antigens, and immunoglobulin preparations, while podofilox is used as an antimitotic drug. A group of compounds, like parbendazole, mebendazole, albendazole, oxibendazole, and cyclobendazole, inhibit angiogenesis with different potencies. Therefore, this high-content angiogenesis assay is promising for profiling angiogenesis inhibitors.

Identification of Angiogenesis Inhibitors That Are Involved in HIF-1α and NF-κB Pathways

To explore the involvement of these identified inhibitors in the HIF-1α and NF-κB signaling pathways, we tested these compounds in cell-based reporter gene assays. Among 50 angiogenesis inhibitors, there were 29 compounds identified from the HRE-bla assay and 14 compounds were confirmed in the HIF-1α–NanoLuc reporter gene assay. There were 24 and 29 compounds identified from the NF-κB β-lactamase and luciferase reporter gene assays, respectively; 17 compounds were confirmed in both assays. The IC_{50} and efficacy for the 50 compounds, as well as cell viability, are summarized for angiogenesis, HIF-1α, and NF-κB assays (**Suppl. Table S1**). The
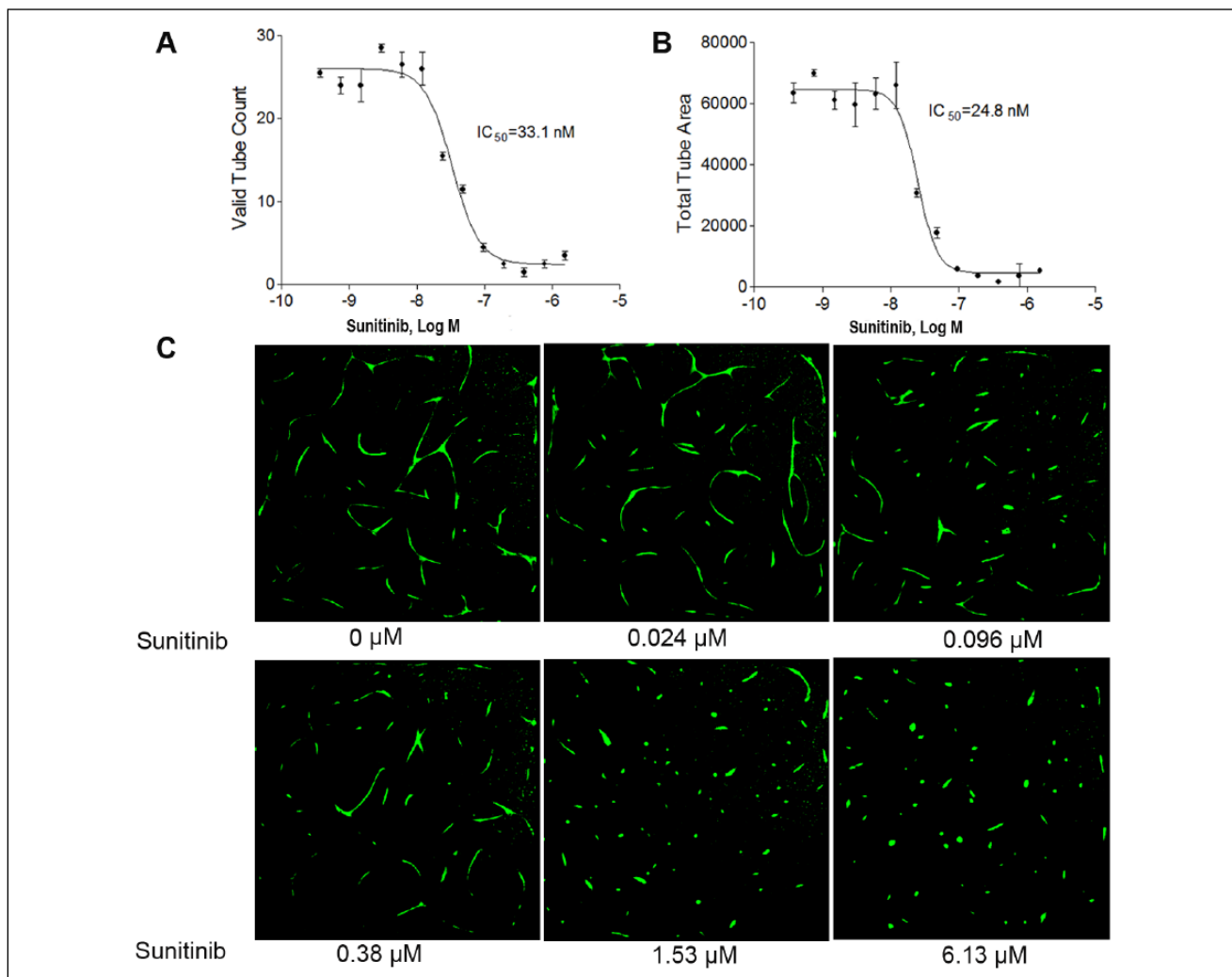
Figure 2. Effect of sunitinib on angiogenesis inhibition in 1536-well plates. Concentration–response curves of sunitinib after a 48 h treatment using (**A**) valid tube count and (**B**) total tube area. Each value represents the mean ± SD of three independent experiments. (**C**) Representative images of GFP-labeled angiogenesis tube formation in the absence or presence of sunitinib. The images were acquired using an ArrayScan VTI reader with a 5× objective. Excitation: 488 nm; emission: 530 nm.

heatmap gives a simultaneous visualization of the compound's potency and efficacy in angiogenesis and HIF-1α and NF-κB pathways (**Fig. 4**). Some compounds, such as actinomycin D, bortezomib, and digitoxin, can inhibit both HIF-1α and NF-κB pathway assays. Concentration–response curves for two novel inhibitors, thimerosal and podofilox, are displayed in **Figure 5**. Thimerosal was confirmed to be involved in the NF-κB pathway using NF-κB β-lactamase and luciferase assays. Our results indicated that the HIF-1α and NF-κB signaling pathways were the major mediators of angiogenesis inhibition.

Discussion

The study reported here utilizes a combined cell-based co-culture with quantitative high-throughput and high-content approaches for the primary screening of compounds that inhibit angiogenesis. Specifically, we used a co-culture of hTERT-immortalized and mesenchymal stem cells and GFP-expressing aortic ECs to allow real-time visualization of angiogenesis regardless of donor variability. The transformed hTERT-MSCs have been validated via colocalization of GFP fluorescence and staining with αSMA, a physiologically relevant marker of smooth muscle cells. Two measurement parameters, valid tube count and total tube area, were optimized and selected for quantitative evaluation of tube formation inhibition. Sunitinib, a known angiogenesis inhibitor, has concentration–response inhibitory effects on tube formation. In our study, we optimized the assays in a 1536-well format, offering the advantage of larger lot size and assay consistency.

The assay was validated by screening the NPC library. The assay performed well in identifying angiogenesis

Table 1. List of Angiogenesis Inhibitors with Known Mechanism.

| Compounds	IC$_{50}$ (μM)	Mechanism of Action	Reference
Albendazole	0.64 ± 0.12	Inhibition of VEGFR-2	39
Bortezomib	0.02 ± 0.004	Inhibition of VEGF and IL-6 secretion	36
C.I. 1040	0.10 ± 0.04	Inhibition of ERK-MAPK signaling	42
Cantharidin	0.38 ± 0.13	Suppression of VEGF-induced JAK1/STAT3, ERK, and AKT	43
Carfilzomib	11.40 ± 0.84	Inhibition of NF-κB activation	44
Clofarabine	0.26 ± 0.03	Inhibition of human EC proliferation	45
Digitoxin	0.03 ± 0.01	Inhibition of HIF-1α synthesis	46
Docetaxel	0.0025 ± 0.0008	JNK2/PHD1 signaling-mediated HIF-1α degradation	35
Emetine	1.80 ± 0.33	Degradation of HIF-2α	47
Flavopiridol hydrochloride	0.80 ± 0.17	Inhibition of HIF-1α	48
Gemcitabine hydrochloride	0.04 ± 0.01	Induction of thrombospondin-1	49
Mebendazole	1.97 ± 0.46	Inhibition of VEGFR-2 kinase	38
Mitomycin C	0.50 ± 0.10	Mitosis inhibitor	50
Mycophenolic acid	0.19 ± 0.05	Cell invasion/migration, tube formation	51
Pazopanib	0.06 ± 0.03	VEGFR-2 inhibition	52
PP242	1.85 ± 0.40	Inhibition of the PI3K/AKT/mTOR pathway	53
Proscillaridin	0.003 ± 0.0006	Inhibition of synthesis of both HIF-1α and HIF-2α	40
Selumetinib	0.08 ± 0.01	Modulation of p-ERK/c-Fos/HIF-1α/VEGF integrated signal pathways	54
Topotecan hydrochloride	0.03 ± 0.01	Inhibition of HIF-1α and HIF-2α accumulation	34
Vatalanib	0.20 ± 0.07	Inhibition of VEGFR	55
Vinblastine sulfate	0.05 ± 0.02	Block microtubule formation	56
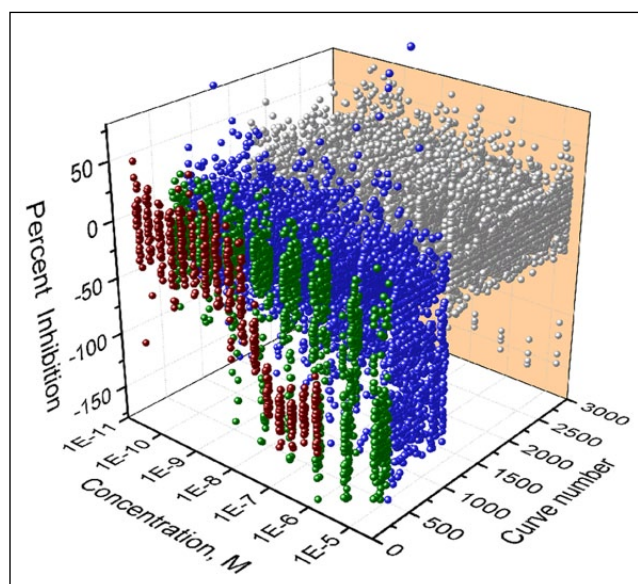
Figure 3. qHTS concentration–response data binned into curve classes. Concentration–response curves for 2816 substances tested, including all the replicates. Concentration–response curves of the positive control, sunitinib (dark red color); compounds with curve classes −1.1, −1.2, and −2.1 (green color); and compounds with curve classes −1.3, −1.4, −2.2, −2.3, −2.4, and −3 (blue color). The inactive compounds are classed as curve class 4, shown in gray.

inhibitors with a Z′ factor value of 0.32. Despite the fact that Z′ > 0.5 has been regarded as a de facto cutoff for most high-throughput screens, $0 < Z′ \leq 0.5$ is often acceptable for complex HCS assays.[33] Out of approximately 2500 drugs screened, 50 drugs were validated to inhibit angiogenesis. These drugs include known angiogenesis inhibitors, like topotecan hydrochloride,[34] docetaxel,[35] and bortezomib.[36] Several novel compounds, such as podofilox, thimerosal, and maduramicin ammonium, were identified to be potential angiogenesis inhibitors. Twenty-one compounds with known mechanisms that inhibit angiogenesis have been summarized (**Table 1**), and their IC$_{50}$ measurements were consistent with those of previous studies. Most of the listed compounds inhibited angiogenesis by affecting VEGF and HIF-1α pathways that are main regulators of angiogenesis.[37] In addition, a group of compounds, including parbendazole, mebendazole, albendazole, and oxibendazole, were all shown to inhibit angiogenesis. Mebendazole and albendazole have been reported to regulate angiogenesis through inhibition of VEGFR-2,[38,39] and the mechanisms of oxibendazole, parbendazole, and oxibendazole in inhibiting angiogenesis remain to be elucidated. These compounds have different potencies in inhibiting angiogenesis, and the variation is probably due to the different functional groups in each compound's structure.

The HIF-1α pathway is a master regulator of angiogenesis; modulation of this pathway could provide a therapeutic benefit for cancer.[40] Inhibitors of the NF-κB pathway are also being developed for treating cancer.[41] Of the 50 identified angiogenesis inhibitors, 14 and 17 compounds were
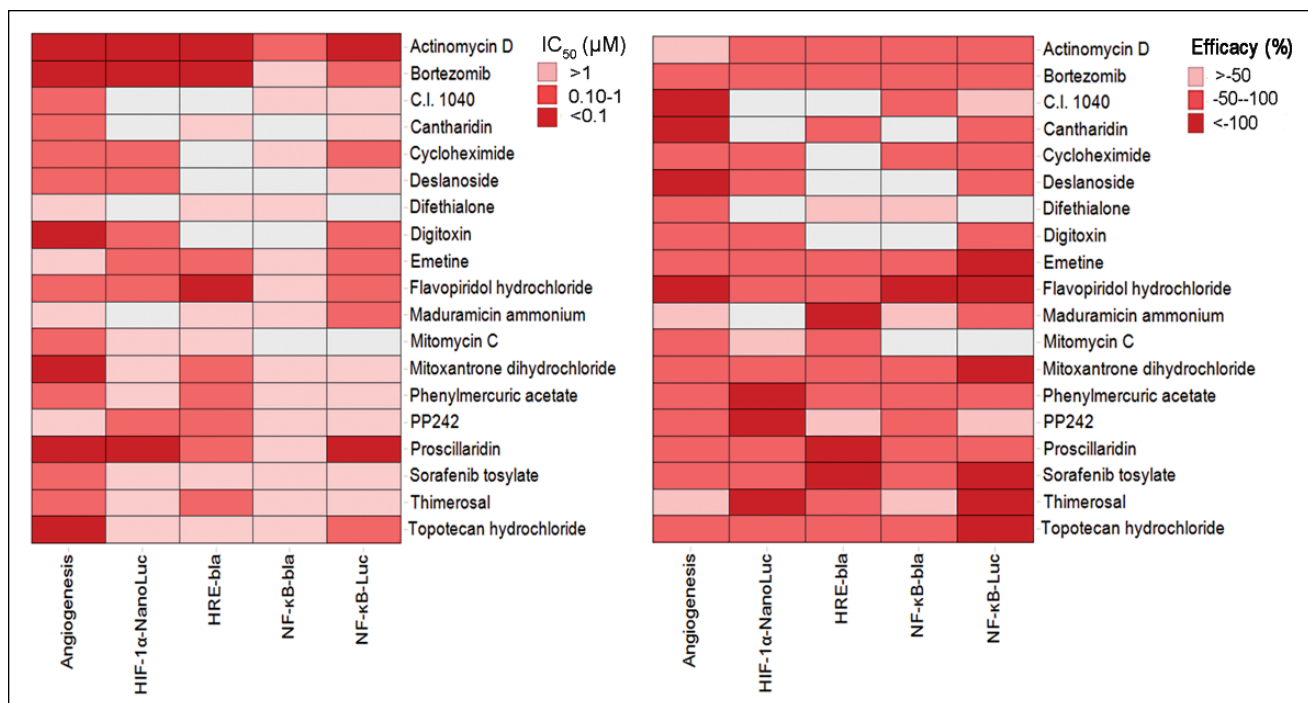
Figure 4. Heatmap of 19 angiogenesis inhibitors involved in the HIF-1α and NF-κB pathways. The drug activity in each cell line is colored according to potency (IC$_{50}$) and efficacy. Inactive compounds are colored in white.
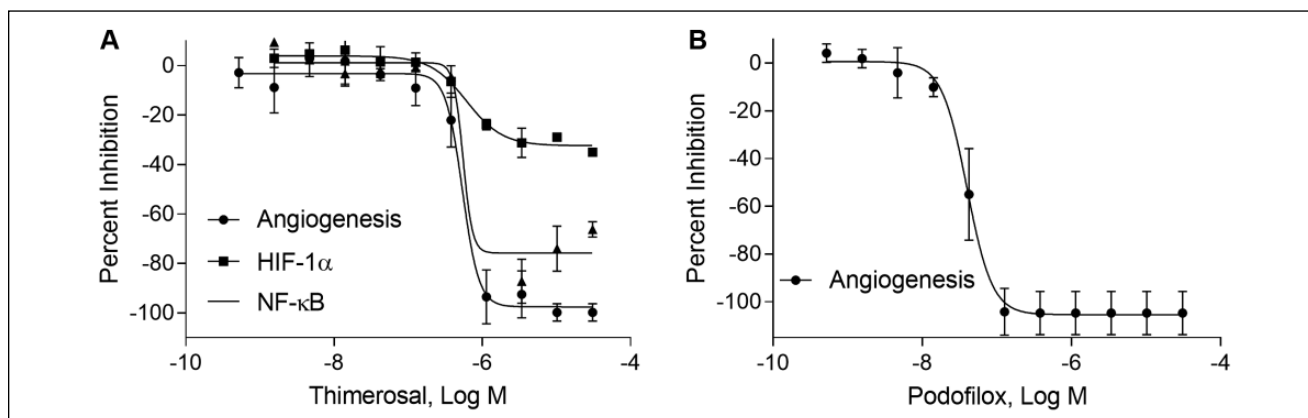

Figure 5. Compound effects on angiogenesis formation and HIF-1α and NF-κB signaling pathways. Concentration–response inhibitory curves of (**A**) thimerosal and (**B**) podofilox. Each data point is expressed as mean ± SD from three experiments.

confirmed to be involved in the HIF-1α and NF-κB pathways, respectively. The profile of HIF-1α inhibitors is comparable to that of a previous study.[29] A group of known HIF-1α inhibitors, like cycloheximide and topotecan, were validated in our study. The mechanism of action by which thimerosal modulates the HIF-1α and NF-κB pathways and the mechanism by which podofilox inhibits angiogenesis remain to be elucidated. We can see that the HIF-1α pathway and NF-κB pathway are closely related to angiogenesis. In all, the co-culture-based high-content angiogenesis assay is promising for the profiling of angiogenesis inhibitors, as well as for studies of vascular biology, drug screening, and tissue engineering.

Declaration of Conflicting Interests

Funding

References

1. Hanahan, D.; Weinberg, R. A. Hallmarks of Cancer: The Next Generation. *Cell* **2011**, *144* (5), 646–674.

2. Ferrara, N.; Kerbel, R. S. Angiogenesis as a Therapeutic Target. *Nature* **2005**, *438* (7070), 967–974.

3. Ellis, L. M.; Hicklin, D. J. VEGF-Targeted Therapy: Mechanisms of Anti-Tumour Activity. *Nat. Rev. Cancer* **2008**, *8* (8), 579–591.

4. Hurwitz, H.; Fehrenbacher, L.; Novotny, W.; et al. Bevacizumab Plus Irinotecan, Fluorouracil, and Leucovorin for Metastatic Colorectal Cancer. *N. Engl. J. Med*. **2004**, *350* (23), 2335–2342.

5. Kane, R. C.; Farrell, A. T.; Saber, H.; et al. Sorafenib for the Treatment of Advanced Renal Cell Carcinoma. *Clin. Cancer. Res*. **2006**, *12* (24), 7271–7278.

6. Goodman, V. L.; Rock, E. P.; Dagher, R.; et al. Approval Summary: Sunitinib for the Treatment of Imatinib Refractory or Intolerant Gastrointestinal Stromal Tumors and Advanced Renal Cell Carcinoma. *Clin. Cancer. Res*. **2007**, *13* (5), 1367–1373.

7. Sternberg, C. N.; Davis, I. D.; Mardiak, J.; et al. Pazopanib in Locally Advanced or Metastatic Renal Cell Carcinoma: Results of a Randomized Phase III Trial. *J. Clin. Oncol*. **2010**, *28* (6), 1061–1068.

8. Donovan, D.; Brown, N. J.; Bishop, E. T.; et al. Comparison of Three In Vitro Human 'Angiogenesis' Assays with Capillaries Formed In Vivo. *Angiogenesis* **2001**, *4* (2), 113–121.

9. Staton, C. A.; Reed, M. W.; Brown, N. J. A Critical Analysis of Current In Vitro and In Vivo Angiogenesis Assays. *Int. J. Exp. Pathol*. **2009**, *90* (3), 195–221.

10. Staton, C. A.; Stribbling, S. M.; Tazzyman, S.; et al. Current Methods for Assaying Angiogenesis In Vitro and In Vivo. *Int. J. Exp. Pathol*. **2004**, *85* (5), 233–248.

11. Moshinsky, D. J.; Ruslim, L.; Blake, R. A.; et al. A Widely Applicable, High-Throughput TR-FRET Assay for the Measurement of Kinase Autophosphorylation: VEGFR-2 as a Prototype. *J. Biomol. Screen*. **2003**, *8* (4), 447–452.

12. Yauch, R. L.; Kadel, E. E., 3rd; Nicholas, C.; et al. Transcriptional-Based Screens for Pathway-Specific, High-Throughput Target Discovery in Endothelial Cells. *J. Biomol. Screen*. **2004**, *9* (8), 704–711.

13. Huynh, Q. K.; Wise, S. J.; Koch, K. A.; et al. Screening and Identification of a Novel Class of TGF-Beta Type 1 Receptor Kinase Inhibitor. *J. Biomol. Screen*. **2011**, *16* (7), 724–733.

14. Kung, A. L.; Zabludoff, S. D.; France, D. S.; et al. Small Molecule Blockade of Transcriptional Coactivation of the Hypoxia-Inducible Factor Pathway. *Cancer Cell* **2004**, *6* (1), 33–43.

15. Lee, Y.; Kang, D. K.; Chang, S. I.; et al. High-Throughput Screening of Novel Peptide Inhibitors of an Integrin Receptor from the Hexapeptide Library by Using a Protein Microarray Chip. *J. Biomol. Screen*. **2004**, *9* (8), 687–694.

16. Ji, D. B.; Zhu, H. B.; Ye, J.; et al. Establishment of a Cell-Based Assay to Screen Regulators of the Hypoxia-Inducible Factor-1-Dependent Vascular Endothelial Growth Factor Promoter. *Biol. Pharm. Bull*. **2008**, *31* (12), 2255–2259.

17. Xia, M. H.; Huang, R. L.; Sun, Y.; et al. Identification of Chemical Compounds That Induce HIF-1 Alpha Activity. *Toxicol. Sci*. **2009**, *112* (1), 153–163.

18. Smirnova, N. A.; Rakhman, I.; Moroz, N.; et al. Utilization of an In Vivo Reporter for High Throughput Identification of Branched Small Molecule Regulators of Hypoxic Adaptation. *Chem. Biol*. **2010**, *17* (4), 380–391.

19. Johnson, R. L.; Huang, R.; Jadhav, A.; et al. A Quantitative High-Throughput Screen for Modulators of IL-6 Signaling: A Model for Interrogating Biological Networks Using Chemical Libraries. *Mol. Biosyst*. **2009**, *5* (9), 1039–1050.

20. Takahashi, T.; Kimura, Y.; Saito, R.; et al. An In Vitro Test to Screen Skin Sensitizers Using a Stable THP-1-Derived IL-8 Reporter Cell Line, THP-G8. *Toxicol. Sci*. **2011**, *124* (2), 359–369.

21. Cash, J. N.; Angerman, E. B.; Kirby, R. J.; et al. Development of a Small-Molecule Screening Method for Inhibitors of Cellular Response to Myostatin and Activin A. *J. Biomol. Screen*. **2013**, *18* (7), 837–844.

22. Li, X.; Yang, J.; He, X.; et al. Identification of Upregulators of BMP2 Expression via High-Throughput Screening of a Synthetic and Natural Compound Library. *J. Biomol. Screen*. **2009**, *14* (10), 1251–1256.

23. Mousseau, Y.; Mollard, S.; Qiu, H.; et al. In Vitro 3D Angiogenesis Assay in Egg White Matrix: Comparison to Matrigel, Compatibility to Various Species, and Suitability for Drug Testing. *Lab. Invest*. **2014**, *94* (3), 340–349.

24. Zanella, F.; Lorens, J. B.; Link, W. High Content Screening: Seeing Is Believing. *Trends Biotechnol*. **2010**, *28* (5), 237–245.

25. Evensen, L.; Micklem, D. R.; Link, W.; et al. A Novel Imaging-Based High-Throughput Screening Approach to Anti-Angiogenic Drug Discovery. *Cytometry A* **2010**, *77* (1), 41–51.

26. Prigozhina, N. L.; Heisel, A.; Wei, K.; et al. Characterization of a Novel Angiogenic Model Based on Stable, Fluorescently Labelled Endothelial Cell Lines Amenable to Scale-Up for High Content Screening. *Biol. Cell* **2011**, *103* (10), 467–481.

27. Huang, R.; Southall, N.; Wang, Y.; et al. The NCGC Pharmaceutical Collection: A Comprehensive Resource of Clinically Approved Drugs Enabling Repurposing and Chemical Genomics. *Sci. Transl. Med*. **2011**, *3* (80), 80ps16.

28. Xia, M. H.; Bi, K.; Huang, R. L.; et al. Identification of Small Molecule Compounds That Inhibit the HIF-1 Signaling Pathway. *Mol. Cancer* **2009**, *8*, 117.

29. Hsu, C. W.; Huang, R.; Khuc, T.; et al. Identification of Approved and Investigational Drugs That Inhibit Hypoxia-Inducible Factor-1 Signaling. *Oncotarget* **2016**, *7* (7), 8172–8183.

30. Miller, S. C.; Huang, R.; Sakamuru, S.; et al. Identification of Known Drugs That Act as Inhibitors of NF-kappaB Signaling

and Their Mechanism of Action. *Biochem. Pharmacol.* **2010**, *79* (9), 1272–1280.

31. Inglese, J.; Auld, D. S.; Jadhav, A.; et al. Quantitative High-Throughput Screening: A Titration-Based Approach That Efficiently Identifies Biological Activities in Large Chemical Libraries. *Proc. Natl. Acad. Sci. U. S. A.* **2006**, *103* (31), 11473–11478.

32. Huang, R.; Xia, M.; Cho, M. H.; et al. Chemical Genomics Profiling of Environmental Chemical Modulation of Human Nuclear Receptors. *Environ. Health Perspect.* **2011**, *119* (8), 1142–1148.

33. Bray, M. A.; Carpenter, A. Advanced Assay Development Guidelines for Image-Based High Content Screening and Analysis. In *Assay Guidance Manual*; Sittampalam, G. S.; Coussens, N. P.; Brimacombe, K.; et al., Eds.; Eli Lilly & Company and the National Center for Advancing Translational Sciences: Bethesda, MD, 2004.

34. Puppo, M.; Battaglia, F.; Ottaviano, C.; et al. Topotecan Inhibits Vascular Endothelial Growth Factor Production and Angiogenic Activity Induced by Hypoxia in Human Neuroblastoma by Targeting Hypoxia-Inducible Factor-1alpha and -2alpha. *Mol. Cancer Ther.* **2008**, *7* (7), 1974–1984.

35. Oh, E. T.; Kim, C. W.; Kim, S. J.; et al. Docetaxel Induced-JNK2/PHD1 Signaling Pathway Increases Degradation of HIF-1alpha and Causes Cancer Cell Death under Hypoxia. *Sci. Rep.* **2016**, *6*, 27382.

36. Roccaro, A. M.; Hideshima, T.; Raje, N.; et al. Bortezomib Mediates Antiangiogenesis in Multiple Myeloma via Direct and Indirect Effects on Endothelial Cells. *Cancer Res.* **2006**, *66* (1), 184–191.

37. Pugh, C. W.; Ratcliffe, P. J. Regulation of Angiogenesis by Hypoxia: Role of the HIF System. *Nat. Med.* **2003**, *9* (6), 677–684.

38. Bai, R. Y.; Staedtke, V.; Rudin, C. M.; et al. Effective Treatment of Diverse Medulloblastoma Models with Mebendazole and Its Impact on Tumor Angiogenesis. *Neuro Oncol.* **2015**, *17* (4), 545–554.

39. Pourgholami, M. H.; Khachigian, L. M.; Fahmy, R. G.; et al. Albendazole Inhibits Endothelial Cell Migration, Tube Formation, Vasopermeability, VEGF Receptor-2 Expression and Suppresses Retinal Neovascularization in ROP Model of Angiogenesis. *Biochem. Biophys. Res. Commun.* **2010**, *397* (4), 729–734.

40. Krock, B. L.; Skuli, N.; Simon, M. C. Hypoxia-Induced Angiogenesis: Good and Evil. *Genes Cancer* **2011**, *2* (12), 1117–1133.

41. Loboda, A.; Stachurska, A.; Florczyk, U.; et al. Activation of HIF-1 Diminishes Activity of Nrf2, NF-kB and AP-1 and Decreases Expression of IL-8 in Endothelial Cells. *FEBS J.* **2009**, *276*, 241.

42. Mavria, G.; Vercoulen, Y.; Yeo, M.; et al. ERK-MAPK Signaling Opposes Rho-Kinase to Promote Endothelial Cell Survival and Sprouting during Angiogenesis. *Cancer Cell* **2006**, *9* (1), 33–44.

43. Wang, T.; Liu, J.; Xiao, X. Q. Cantharidin Inhibits Angiogenesis by Suppressing VEGF-Induced JAK1/STAT3, ERK and AKT Signaling Pathways. *Arch. Pharm. Res.* **2015**, *38* (2), 282–289.

44. Tang, W.; Su, G.; Li, J.; et al. Enhanced Anti-Colorectal Cancer Effects of Carfilzomib Combined with CPT-11 via Downregulation of Nuclear Factor-Kappab In Vitro and In Vivo. *Int. J. Oncol.* **2014**, *45* (3), 995–1010.

45. Anshu, M.; Roy, R. L.; Qu, Z. Antiangiogenic Activity of Clofarabine. *AACR Meet. Abstr.* **2006**, *66*, 55–56.

46. Zhang, H.; Qian, D. Z.; Tan, Y. S.; et al. Digoxin and Other Cardiac Glycosides Inhibit HIF-1alpha Synthesis and Block Tumor Growth. *Proc. Natl. Acad. Sci. U.S.A.* **2008**, *105* (50), 19579–19586.

47. Kong, H. S.; Lee, S.; Beebe, K.; et al. Emetine Promotes von Hippel-Lindau-Independent Degradation of Hypoxia-Inducible Factor-2alpha in Clear Cell Renal Carcinoma. *Mol. Pharmacol.* **2010**, *78* (6), 1072–1078.

48. Newcomb, E. W. Flavopiridol: Pleiotropic Biological Effects Enhance Its Anti-Cancer Activity. *Anticancer Drugs* **2004**, *15* (5), 411–419.

49. Laquente, B.; Lacasa, C.; Ginesta, M. M.; et al. Antiangiogenic Effect of Gemcitabine Following Metronomic Administration in a Pancreas Cancer Model. *Mol. Cancer Ther.* **2008**, *7* (3), 638–647.

50. Pepper, M. S.; Ferrara, N.; Orci, L.; et al. Leukemia Inhibitory Factor (LIF) Inhibits Angiogenesis In Vitro. *J. Cell Sci.* **1995**, *108* (Pt. 1), 73–83.

51. Domhan, S.; Muschal, S.; Schwager, C.; et al. Molecular Mechanisms of the Antiangiogenic and Antitumor Effects of Mycophenolic Acid. *Mol. Cancer Ther.* **2008**, *7* (6), 1656–1668.

52. Hamberg, P.; Verweij, J.; Sleijfer, S. (Pre-)Clinical Pharmacology and Activity of Pazopanib, a Novel Multikinase Angiogenesis Inhibitor. *Oncologist* **2010**, *15* (6), 539–547.

53. Xing, X.; Zhang, L.; Wen, X.; et al. PP242 Suppresses Cell Proliferation, Metastasis, and Angiogenesis of Gastric Cancer through Inhibition of the PI3K/AKT/mTOR Pathway. *Anticancer Drugs* **2014**, *25* (10), 1129–1140.

54. Gao, J. H.; Wang, C. H.; Tong, H.; et al. Targeting Inhibition of Extracellular Signal-Regulated Kinase Kinase Pathway with AZD6244 (ARRY-142886) Suppresses Growth and Angiogenesis of Gastric Cancer. *Sci. Rep.* **2015**, *5*, 16382.

55. Wood, J. M.; Bold, G.; Buchdunger, E.; et al. PTK787/ZK 222584, a Novel and Potent Inhibitor of Vascular Endothelial Growth Factor Receptor Tyrosine Kinases, Impairs Vascular Endothelial Growth Factor-Induced Responses and Tumor Growth after Oral Administration. *Cancer Res.* **2000**, *60* (8), 2178–2189.

56. Ribatti, D.; Guidolin, D.; Conconi, M. T.; et al. Vinblastine Inhibits the Angiogenic Response Induced by Adrenomedullin In Vitro and In Vivo. *Oncogene* **2003**, *22* (41), 6458–6461.